

## ESTIMATION OF CLINICAL SIZE OF BREAST TUMOUR LESIONS USING CONTRAST ENHANCED MAGNETIC RESONANCE IMAGING: DELINEATION OF TUMOUR BOUNDARIES

Manpreet Singh (1), Manjesh Dalal (2), Gurasis Singh Sodhi (2)

(1) Department of Mechanical Engineering,  
University of Maryland Baltimore County,  
Baltimore, MD, USA

(2) Government Medical College and Hospital,  
Sector-32B, Chandigarh, India

### INTRODUCTION

Breast Imaging-Reporting and Data System (BI-RADS) classifies breasts into four categories in the order of radiographic breast density composition namely extremely dense (ED)-10% (type-D), heterogeneously dense (HD)-40% (type-C), scattered fibroglandular (SF)-40% (type-B) and predominantly fatty (PF) is reported in about 10% of women (type-A)<sup>1</sup>. Under such classification BI-RADS defines tumour into namely six assessment categories<sup>2</sup>. TNM (Tumour-Node-Metastasis) tool is widely used to describe the stage of tumour. T refers to size of the tumour, N relates to primary inspection whether cancerous cells spread to lymphatic nodes and M explains whether it invades to other organs of the patient. Clinically, the staging of the tumour in the breast may be defined as T1 (size ≤ 20 mm): T1mi (≤ 1 mm), T1a (1 mm < size ≤ 5 mm), T1b (5 mm < size ≤ 10 mm), T1c (10 mm < size ≤ 20 mm); T2 (20 mm < size ≤ 50 mm); T3 (≥ 50 mm); T4a (tumour has grown into chest wall), T4b (tumour has grown into skin), T4c (grown into chest wall and skin), T4d (inflammatory).

The delineation of tumour is defined using three fundamental axioms i.e. tumour volumes<sup>3</sup> namely gross tumour volume (GTV), clinical target volume (CTV), planning target volume (PTV) is critical to design an effective radiotherapy planning or thermal ablation treatment therapy (Radiofrequency Ablation) etc. Hence, the accurate tumour boundaries needs clear demarcation in order to ensure the safety of organs at risk (ORs) considering that the organs must not receive higher-than-safe-dose. Therefore, clinical size of tumour holds a great significance for the tumours such as glioblastoma multiforme (GBM), CWR (Chest Wall Recurrence) etc. where damage to healthy anatomical structures such as spinal cord, chest wall etc., produces a severe clinical manifestation<sup>4</sup>.

### METHODS

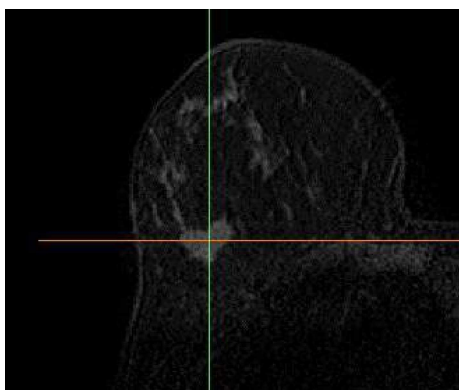
Clinical breast MRI examination was performed at Government Medical College and Hospital, Chandigarh, India in the department of Radiodiagnosis & Imaging with Phillips at magnetic field of 1.5T using a standard and consistent contrast enhanced injections following a clinical breast MRI protocol. MRI uses magnetic fields instead of x-rays to produce very detailed and refined cross-sectional images of the cancerous lesion of breast organ. Six Woman were imaged in the prone position using a dedicated multichannel surface array breast coil. After the native scan was obtained, Contrast Enhanced sequences (CE) were acquired in axial plane employing 3D T1-weighted fast gradient echo-based DCE series with one pre and three post-gadolinium contrast-enhanced sequences. MRI exams for breast imaging use a contrast material (usually gadolinium-DTPA) that was injected into a vein in the arm before or during the exam to improve the ability to capture detailed images of breast tissue. The DICOM format information about both breasts including other organs was captured. The nearest neighbor of tumour (subpart node T) node corresponds to the node  $i$  in the breast (object) mesh having the minimum Euclidean distance (ED) to the tumour node via eq. 1 as:

$$ED = \sqrt{(x_{nodeT} - x_i)^2 + (y_{nodeT} - y_i)^2 + (z_{nodeT} - z_i)^2} \quad (1)$$

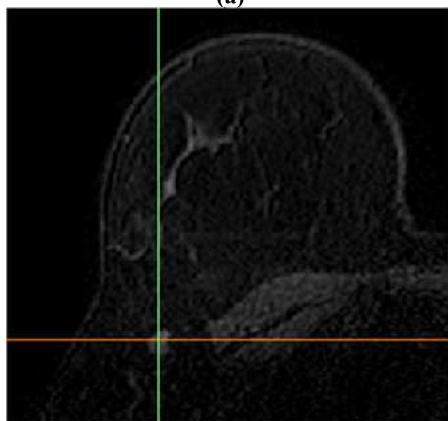
where,  $x, y, z$  represents the nodal coordinates. It is ensured that tumour offers a higher level of refinement compared with the mesh for the breast anatomy as a single unit.

### RESULTS

Fig. 1 illustrates one slice from a set of 1051 images of DCE-MRI acquisition. In the first case scenario, the breast composition is found to resemble a case of type-A predominantly or entirely fatty breast anatomy. A relatively well defined irregular mass lesion with spiculated



(a)



(b)

**Figure 1:** Case Scenario-1: a) DCE-MRI slice of type-A breast cancerous lesion in axial plane, b) spicule is approaching chest wall.

margins measuring  $19 \times 17 \times 14$  mm in size and appearing isointense to glandular tissue on T2W images and hyperintense on STIR images is noted in the upper outer quadrant of the right breast. The cancerous lesion is reported at a distance of 1.5 cm from the skin at the lateral border of the breast and 1.8 cm from the chest wall. It can be followed from fig. 1b that one of the spicule appears mildly bulky and pulled up and is seen reaching upto the pectoralis muscle. A lymph node measuring  $10 \times 6.3$  mm is also noted in the axilla along the chest wall. Hence, first case is assessed as BI-RADS V (malignant case). Referring to fig. 2, the second case scenario, the breast composition is a case of type-B scattered fibroglandular breast anatomy. STIR hyperintense diffuse subcutaneous thickening measuring 1.3 cm with corresponding mild linear non-mass enhancement curves. It can be coined as a case of BI-RADS IVa. Fig. 3 shows a well circumscribed homogeneously enhancing STIR hyperintense mass lesion measuring  $1.4 \times 0.8$  cm and appearing isointense to glandular tissue on T2W images is noted in retro areolar location in midline with type II enhancement and is a case of BI-RADS IV C. The distance from the skin at anterior surface of the breast is 2.1 cm. Homogeneous internal enhancement is found on post contrast images.

## DISCUSSION

This study covers an extended spectrum of clinical cases (1) to analyze the accurate tumour size, (2) to demarcate accurate tumour boundaries in order to plan an effective target volumes for radiotherapy, thermal ablation including radiofrequency ablation and nanoparticles induced thermal ablation. Once the clinical size of the tumour is established, realistic three-dimensional volume of the tumour can be calculated with its realistic shape and irregular nodal features with the available computational imaging platforms such as MIMICS, 3-matic, Simplewa-

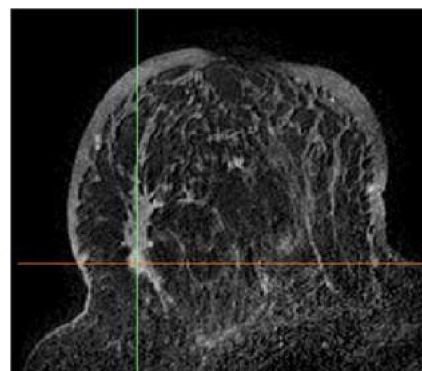


**Figure 2:** Case Scenario-2: Illustration of DCE-MRI slice of type-B breast carcinoma in axial plane.

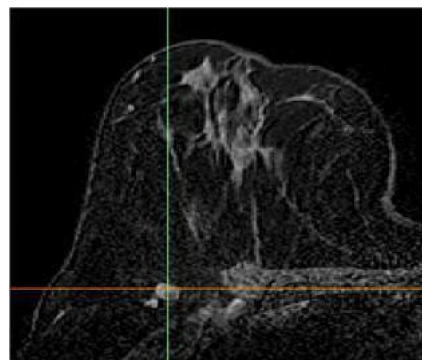


**Figure 3:** Case Scenario-3: Illustration of DCE-MRI slice of type-B breast carcinoma in axial plane.

-re etc. Such domains can be successfully imported into ABAQUS, Comsol-Multiphysics, ANSYS etc. as mesh files to do heat transfer analysis or run Monte-carlo simulations for effective radiation planning. Accurate margins (0.5 cm-1 cm) can only be sacrificed if true tumour boundaries with irregular spread can be retrieved. Hence, this study helps in enhancing the treatment efficacy of cancer treatments and thereby designing protocols for radiation, thermal ablation and hyperthermia therapies. As used in first case scenario, the high resolution data with slice thickness equivalent to 0.5 mm or lesser must be used in order to capture the detailed anatomical features and pathology of tumour. The future effort in this direction would be to capture the blood supplying vessels to the tumour using MRI-Angiogram although not commonly used in imaging.

## ACKNOWLEDGEMENTS

Manpreet Singh is appreciative of the Graduate School, University of Maryland, Baltimore County for conferring the award of Dissertation Fellowship towards the progress of Doctorate degree. M. Dalal and G. S. Sodhi are thankful to the GMCH Sec-32B, Chandigarh for sharing the patient's data following institutional approval. It is also ensured that the details of the patients used for this primary analysis is kept highly confidential and will not be disclosed in any forum except using it for analysis, research and computational purpose.

## REFERENCES

- [1] <https://www.cancer.gov/types/breast/breast-changes/dense-breasts>
- [2] <https://radiopaedia.org/articles/breast-imaging-reporting-and-data-system-bi-rads-assessment-category-6>.
- [3] Burnet, N.G. et al., *Cancer Imaging*, 4:153-161, 2004.
- [4] Vaupel, P et al., *Pathophysiol. of solid tumour*, *Springer* 51-92, 2009